Journal of Molecular Graphics and Modelling 51 (2014) 7–12

Contents lists available at ScienceDirect

Journal of Molecular Graphics and Modelling

journal homepage: www.elsevier.com/locate/JMGM

Design of novel camphane-based derivatives with antimycobacterial activity

Georgi Stavrakov[a], Violeta Valcheva[b], Irena Philipova[c], Irini Doytchinova[a,*]

[a] Faculty of Pharmacy, Medical University of Sofia, 2 Dunav st., Sofia 1000, Bulgaria
[b] Institute of Microbiology, Bulgarian Academy of Sciences, 26 Akad. Bonchev st., Sofia 1113, Bulgaria
[c] Institute of Organic Chemistry, Bulgarian Academy of Sciences, 9 Acad. Bonchev st., Sofia 1113, Bulgaria

ARTICLE INFO

Article history:
Accepted 21 April 2014
Available online 30 April 2014

Keywords:
Tuberculosis
Antimycobacterial activity
Camphane-based derivatives
QSAR
Drug design

ABSTRACT

Although tuberculosis (TB) continues to be one of the leading infectious disease killers globally, it is curable and preventable. Despite the existence of safe, well tolerated and effective drugs used in the TB treatment, the interest in new entities, combinations and regimens increases during the last 10 years. Recently, we reported for a new class of anti-TB agents – camphane-based derivatives with nanomolar activity against *Mycobacterium tuberculosis* strains. The quantitative structure–activity relationship (QSAR) study on 12 compounds revealed several structural requirements for antimycobacterial activity: two hydrogen bond donors, two or three rings and no large branched substituents. Here, we describe the design of a set of nine novel camphane-based derivatives following these requirements. The compounds were synthesized and tested against *M. tuberculosis* strain H37Rv. Four of them showed activities in the nanomolar range, significantly higher than the activities in the initial set. The QSAR study based on all 21 derivatives pointed to two main structural requirements for anti-TB activity: two hydrogen bond donors and a side chain with aromatic ring.

1. Introduction

Tuberculosis (TB) remains a leading infectious disease killer globally. In Africa, TB is the biggest killer of people with HIV/AIDS [1]. One third of the world's population is thought to have been infected with *Mycobacterium tuberculosis* [2] but about 90% of them have asymptomatic, latent TB infections. TB is curable and preventable. Bacille Calmette Guerin (BCG) is the only vaccine available today for protection against tuberculosis [3]. It is most effective in protecting children from the disease. Many strains of tuberculosis resist the drugs mostly used to treat the disease. People with active tuberculosis must take several types of medications for many months to eradicate the infection and to prevent the development of antibiotic resistance [4].

After 40 years of neglect, encouraging advances have been made in TB drug research and development during the last 10 years, resulting in nine compounds currently under clinical development and more than 20 new chemical entities in preclinical research [5]. New drugs and drug combinations are needed that have strong, bactericidal activity against various strains of *M. tuberculosis*.

When the target is known, structure-based methods as docking, molecular dynamics simulations, virtual screening, de novo design, are effective in lead identification and lead optimization [6]. When the initial information comes from a whole-cell experiment, ligand-based methods as pharmacophore search, 2D and 3D QSAR studies, fingerprints and similarity search, are helpful in the design of new ligands [6]. The advances in the chase of new anti-TB drugs have been recently reviewed [7]. The ligand-based methods are involved actively [8–18] but the structure-based methods targeting specific *M. tuberculosis* enzymes also take place [19–22].

Recently, we synthesized a series of novel camphane-based derivatives and tested them against two *M. tuberculosis* strains: strain H37Rv and multi-drug resistant strain 43 [23]. All of them were active against strain H37Rv with *MIC* values in the micro- and nanomolar range. Three derivatives showed also activity against MDR strain 43 with *MIC* values in the micromolar range. A detailed QSAR study was conducted and the following 2D-QSAR model was derived:

$$pMIC = 0.592knotp - 0.445SHHBd - 0.683nrings + 12.992,$$

$$n = 12, \quad r^2 = 0.875, \quad SEE = 0.290, \quad F = 18.58, \quad q^2 = 0.675$$

The structures of the compounds, their experimental *MIC* and *pMIC* ($-\log MIC$) are given in Table 1. In Table 1 also are given the values of the descriptors presented in the model and the calculated *pMIC* and *MIC*. The descriptor *knotp* relates to intermolecular accessibility [24]. Negative *knotp* values correspond to large molecules

* Corresponding author. Tel.: +359 9236506.
E-mail address: idoytchinova@pharmfac.net (I. Doytchinova).

http://dx.doi.org/10.1016/j.jmgm.2014.04.008
1093-3263/

Table 1
Structure, experimental *MIC*s, molecular descriptors and calculated *MIC*s of the training set.

Cmpd.[a]	Structure	*MIC(exp)* (μM)	*pMIC(exp)*	*knotp*	*SHHBd*	*nrings*	*pMIC(calc)*	Residual
1 (**3a**)	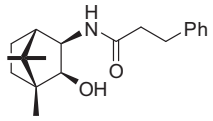	0.33	6.481	−4.109	4.327	3	6.584	−0.103
2 (**3b**)	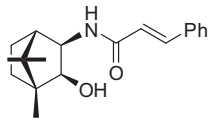	0.33	6.481	−4.109	4.382	3	6.559	−0.078
3 (**3c**)	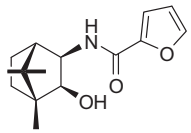	0.38	6.420	−4.385	4.432	3	6.373	0.047
4 (**3d**)	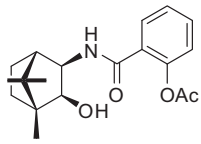	0.30	6.523	−4.475	4.523	3	6.280	0.243
5 (**3e**)	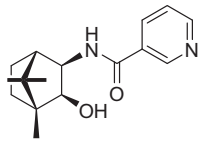	0.36	6.444	−4.385	4.416	3	6.381	0.063
6 (**4**)	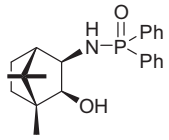	13.55	4.868	−5.506	4.553	4	4.941	−0.073
7 (**5**)	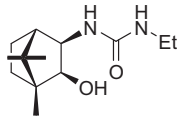	0.41	6.387	−3.880	6.026	2	6.646	−0.259
8 (**9a**)	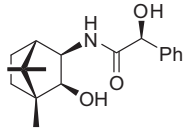	16.50	4.783	−4.810	7.105	3	4.932	−0.149
9 (**9b**)	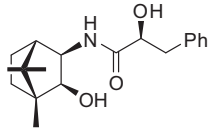	6.30	5.201	−4.606	7.049	3	5.078	0.124
10 (**9c**)	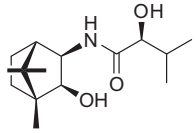	0.74	6.131	−4.784	6.899	2	5.722	0.409
11 (**9d**)	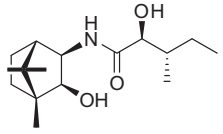	7.06	5.151	−4.907	6.915	2	5.643	−0.492
12 (**9e**)	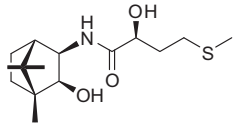	0.66	6.180	−4.434	6.939	2	5.912	0.268

[a] The compounds ID according to Ref. [23] are given in parenthesis.

Table 2
Structure, molecular descriptors, predicted and experimental *MIC*s of the designed compounds.

Cmpd.	Structure	*knotp*	*SHHBd*	*nrings*	*pMIC(pred)*	*pMIC(exp)*	Residual	*MIC(exp)* (μM)
13	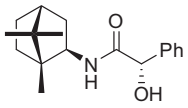	−4.417	4.472	3	6.337	6.770	0.433	0.17
14	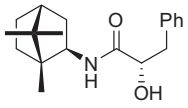	−4.212	4.420	3	6.481	6.796	0.315	0.16
15	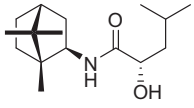	−3.837	4.301	2	7.439	5.126	−2.313	7.48
16	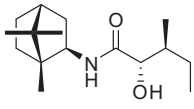	−4.513	4.308	2	7.036	5.126	−1.910	7.48
17	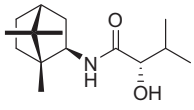	−4.390	4.294	2	7.115	5.103	−2.012	7.89
18	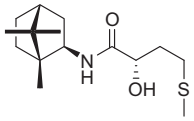	−4.041	4.327	2	7.307	6.770	−0.537	0.17
19	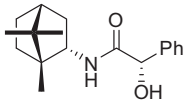	−4.417	4.472	3	6.337	5.008	−1.329	9.96
20	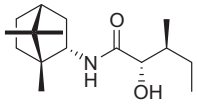	−4.513	4.308	2	7.036	4.728	−2.308	18.70
21	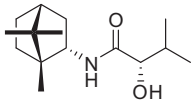	−4.390	4.294	2	7.115	6.699	−0.416	0.20

with high degree of branching, distal substituents, or adjacent (conjugated) rings. Such substituents are unfavorable for antimycobacterial activity. The descriptor *SHHBd* represents the sum of atom-type hydrogen E-state indices for hydrogen bond donors. There are two common hydrogen bond donors in the side chain of the studied structures: the OH and NH groups. Any additional H-bond donor decreases the activity. The descriptor *nrings* accounts for the number of rings in the molecular graph. It has a negative contribution; therefore, the presence of many rings in the structure decreases the activity. The camphene moiety itself brings two rings. One additional ring in the side chain is well tolerated. However, four rings in the structure (compound **6**) drastically decrease the activity.

In the present study, we designed a series of novel camphane-based derivatives following the structural requirements for antimycobacterial activity derived in the previous study. The compounds were synthesized and tested against *M. tuberculosis* strain H37Rv. Four of them showed MICs in the nanomolar range, two times lower than the lowest *MIC* in the initial set. New QSAR studies provide clear directions for further lead optimization of the camphanes as antimycobacterial agents.

2. Results

2.1. Design of novel camphane-based derivatives and prediction of their antimycobacterial activity

Based on the structural requirements derived in the previous study, we designed six new camphane-based derivatives carrying two hydrogen bond donors, two or three rings and no large branched substituents (Table 2). The side chain was attached equatorially (exo) at position 3 in the camphane ring. Additionally, three axial (endo) analogs were designed to test the effect of equatorial/axial position of the side chain on the activity. The antimycobacterial activity of the newly designed compounds was predicted by the QSAR model derived in the previous study. In Table 2 are listed the predicted values for *pMIC* and *MIC*. The predicted activities were in the nanomolar range.

2.2. Synthesis and antimycobacterial activity of the novel camphanes

The newly designed nine camphane-based derivatives were synthesized and tested against *M. tuberculosis* strain H37Rv as described in the Methods section. The experimental *MIC* values are given in Table 2. Four of the compounds have activities in the nanomolar range (compounds **13**, **14**, **18** and **21**) and five of them (compounds **15**, **16**, **17**, **19** and **20**) – in the micromolar range. The highly active derivatives are well predicted with residuals below or around a half log unit. The less active compounds have poor prediction with residuals around or above 2 log units. In order to investigate the reason for the poor prediction, a new QSAR study was performed based on the dataset of all 21 camphanes synthesized in our laboratory.

2.3. Quantitative structure–activity relationships on the whole set

The chemical structure of all studied compounds was described by 178 molecular descriptors computed using the software package MDL QSAR version 2.2 [25]. The descriptors relevant to the antimycobacterial activity of the studied compounds were selected by genetic algorithm (GA) and stepwise regression as described in the Methods section. The best performed model in terms of r^2 and q^2 is given below:

$$pMIC = 1.178knotpv - 1.271SsssCH\_acnt + 14.215, \quad n = 17,$$
$$r^2 = 0.841, \quad SEE = 0.342, \quad F = 36.88, \quad q^2 = 0.692$$

No intercorrelation between the descriptors in the model was observed ($R < 0.7$). The descriptors relevant to the anti-TB activity and the calculated by the model *MIC*s are given in Table 3.

The descriptor *knotpv* is calculated as a difference between χ valence cluster-3 and χ valence path/cluster-4. It correlates with the descriptor *knotp* appeared in our previous QSAR model and has a similar interpretation. The replacement of *knotpv* with *knotp* decreases both r^2 and q^2 of the model. Compounds with branched aliphatic side chains have highly negative values for *knotpv* and low antimycobacterial activities.

The descriptor *SsssCH_acnt* counts the >CH– groups in the molecule, i.e. the number of tertiary carbon atoms. Although it does not correlate with *knotpv*, this descriptor also reflects the degree of branching in the molecules. The camphane moiety itself contains three tertiary carbons. Additionally, compounds with aliphatic side chains have one or two tertiary carbons. The negative coefficient of *SsssCH_acnt* in the model points to the disfavored contribution of this atom to the activity of compounds.

The calculated *pMIC* versus observed *pMIC* are plotted in Fig. 1. The model has four outliers – compounds with residuals higher than 1 log unit. These are compounds **10** and **11** from the training set and compounds **19** and **21** from the newly designed set. Compounds **10**, **11** and **21** are underestimated by the new QSAR model, compound **19** is overestimated. As **19** and **21** are both *endo*-analogs, we included in the model an indicator variable describing the *exo*/*endo* position of the side chain. No improvement of the model was observed.

3. Discussion

In the present study, a QSAR-guided design of nine novel camphane-based derivatives was performed. The compounds were design to include two hydrogen bond donors, two or three rings and no large branched substituents. Additionally, three axial (endo) analogs were designed to test the effect of equatorial/axial position

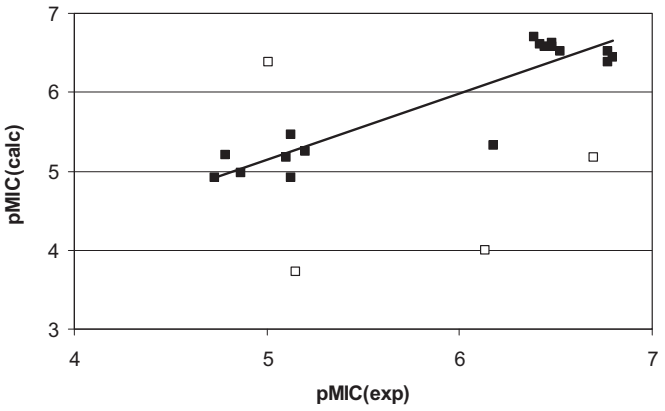

Fig. 1. Calculated vs. observed antimycobacterial activity of the studied compounds. Outliers are given by blank squares.

of the side chain on the activity. The compounds were synthesized and tested for antimycobacterial activity. Four of them showed *MIC* values in the nanomolar range. All of these four *MIC*s were higher than the highest activity in the training set.

The less active compounds have poor prediction with residuals around or above 2 log units. In order to investigate further the structure–activity relationship, a new QSAR study was performed based on the dataset of all 21 camphanes. The newly derived QSAR model confirmed the negative contribution of large branched substituents. Additionally, the negative contribution of the tertiary carbon atoms on the anti-TB activity was revealed.

Two well defined clusters are formed in the graph presented in Fig. 1. The left cluster comprises the low active compounds with *pMIC* values below and around 5. It contains seven structures carrying three hydrogen bond donors or large branched side chains. The ten highly active compounds are clustered on the right side of the plot and have *pMIC* values above 6. Seven of them have aromatic rings and two contain sulfur in the side chain. The addition of an indicator variable accounting for the presence of sulfur does not improve the model.

The model has four outliers. Compounds **10** and **11** are underestimated (*pMIC(exp)* = 6.131 and *pMIC(calc)* = 3.989 for compound **10** and *pMIC(exp)* = 5.151 and *pMIC(calc)* = 3.731 for compound **11**). Both compounds contain three hydrogen bond donors, no aromatic ring and one tertiary carbon atom in the side chain. Additionally, compound **11** carries a large branched substituent.

Compound **19** is overestimated by the model – it has *pMIC(pred)* = 6.337, *pMIC(exp)* = 5.008 and *pMIC(calc)* = 6.388. It is an endo-analog of compound **13**. It contains two hydrogen bond donors, one aromatic ring and no large branched substituents. Compound **21** also is endo-analog but it is underestimated by the model: *pMIC(pred)* = 7.115, *pMIC(exp)* = 6.699 and *pMIC(calc)* = 5.171. It contains two hydrogen bond donors, no aromatic ring and one tertiary carbon atom. There are three endo-analogs in the set: compound **19** is low active in contrast to its high-active exo-analog compound **13** (*pMIC(exp)* = 6.770); compound **20** is low-active (*pMIC(exp)* = 4.728) as its exo-analog compound **16** (*pMIC(exp)* = 5.126), while compound **21** is highly active (*pMIC(exp)* = 6.699) in contrast to its low-active exo-analog compound **17** (*pMIC(exp)* = 5.103). These ambiguous contributions of the endo substituents explain the insignificance of the indicator variable describing the exo/endo position of the side chain.

Summarizing the QSAR studies performed on the two sets of camphane derivatives, one might conclude that a side chain containing aromatic ring is preferred for anti-TB activity instead of aliphatic one even with low branching. Two hydrogen bond donors

Table 3
Experimental *MIC*s, molecular descriptors and calculated *MIC*s of the whole set.

Cmpd.	*MIC(exp)* (μM)	*pMIC(exp)*	*knotpv*	*SsssCH_acnt*	*pMIC(calc)*	Residual
1	0.33	6.481	−3.250	3	6.576	−0.095
2	0.33	6.481	−3.207	3	6.626	−0.145
3	0.38	6.420	−3.219	3	6.612	−0.192
4	0.30	6.523	−3.294	3	6.524	−0.001
5	0.36	6.444	−3.243	3	6.584	−0.140
6	13.55	4.868	−4.604	3	4.981	−0.113
7	0.41	6.387	−3.142	3	6.702	−0.315
8	16.50	4.783	−3.333	4	5.207	−0.424
9	6.30	5.201	−3.294	4	5.252	−0.051
10	0.74	6.131	−3.288	5	3.989	2.142
11	7.06	5.151	−3.507	5	3.731	1.420
12	0.66	6.180	−3.227	4	5.332	−0.848
13	0.17	6.770	−3.303	3	6.388	0.382
14	0.16	6.796	−3.370	3	6.434	0.362
15	7.48	5.126	−3.118	4	5.460	−0.334
16	7.48	5.126	−3.583	4	4.913	0.213
17	7.89	5.103	−3.364	4	5.171	−0.068
18	0.17	6.770	−3.409	3	6.513	0.257
19	9.96	5.008	−3.409	3	6.388	−1.380
20	18.70	4.728	−3.583	4	4.913	−0.185
21	0.20	6.699	−3.364	4	5.171	1.528

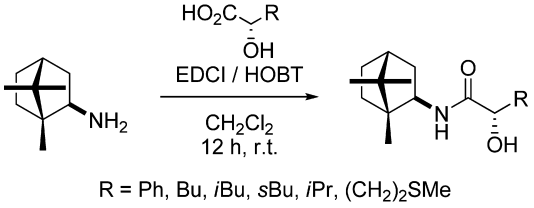

Scheme 1. Synthesis of the newly designed structures.

are optimal for high affinity. Additionally, two of the highly active compounds carry sulfur-containing side chains.

4. Methods

4.1. Synthesis of novel camphane-based derivatives

The detailed synthesis of the newly designed camphane derivatives was described elsewhere [26]. Readily available isobornylamine and bornylamine were selected as the key (+)-camphor-derived starting compounds [27,28]. These amines were attached to a set of α-hydroxy acids, derived from the corresponding α-amino-acids. The amide linkage was accomplished by procedures developed for peptide synthesis (Scheme 1). The reaction was optimized for the commercially available mandelic acid applying *N*-(3-dimethylaminopropyl)-*N′*-ethylcarbodiimide hydrochloride (EDCI), and 1-hydroxybenzotriazole hydrate (HOBT) as coupling reagents. Following the optimized protocol we synthesized amido-alcohols **13**–**21** (Scheme 1) in good yields and excellent purity after flash column chromatography.

*General procedure for the preparation of amides **13**–**21***: 1-Hydroxybenzotriazole (HOBt) (1.1 equiv.) and the respective α-hydroxy acid (1 equiv.) were suspended in dichloromethane, and the mixture was stirred for 5 min. Then, *N*-[3-(dimethylamino)propyl]-*N*-ethylcarbodiimide (EDC) (1.1 equiv.) was added, followed by isobornylamine or bornylamine (1 equiv.). Stirring was continued at room temperature until the starting material was completely consumed (TLC). The mixture was quenched with water, extracted with CH_2Cl_2, washed with 2 M HCl, sat. aq. $NaHCO_3$ and brine. The organic phase was dried over Na_2SO_4, and concentrated under vacuum. The residue was purified by flash column chromatography on silica gel.

4.2. Antimycobacterial activity

The antimycobacterial activity was determined through the proportional method of Canetti toward reference strain *M. tuberculosis* H37Rv [29]. A sterile suspension/solution of each tested compound was added to Löwenstein–Jensen egg based medium before its coagulation (30 min at 85 °C). Each compound was tested at four concentrations – 5 mg/ml, 2 mg/ml, 0.2 mg/ml and 0.1 mg/ml (in DMSO). Tubes with Löwenstein–Jensen medium (5 ml) containing tested compounds and those without them (controls) were inoculated with a suspension of *M. tuberculosis* H37Rv (105 cells/ml) and incubated for 45 days at 37 °C. The ratio between the number of colonies of *M. tuberculosis* grown in medium containing compounds and the number of colonies in control medium were calculated and expressed as percentage of inhibition. The MIC is defined as the minimum concentration of compound required to inhibit bacterial growth completely (0% growth). The MIC values are calculated and given as μM.

4.3. Molecular descriptors

The chemical structure of the studied compounds was described by 178 molecular descriptors computed using the software package MDL QSAR version 2.2 [25]. The descriptors were grouped into five types: molecular connectivity χ (chi) indices [30], which represent molecular structure by encoding significant topological features of whole molecule; κ shape indices – a family of graph-based structure descriptors that represent shape [31]; electrotopological state (E-state) indices, which represent the electron density at each atom and the ability of those electrons to participate in intermolecular interactions [31]; molecular properties – weight, *log P*, *log D7.4*, number of rings, number of hydrogen bond donors and acceptors, etc.; and 3D molecular properties such as polarizability, surface area, volume, etc.

4.4. Variable selection

A genetic algorithm (GA) [32], as implemented in the MDL QSAR package, was used as a variable selection procedure in the present study. GA allows one to select a subset of the most significant predictors using two evolutionary operations: random mutation and genetic recombination (crossover). The algorithm was used in the study with default values for the size of initial population

[32], choice of parents (tournament selection), types of crossover (uniform crossover) and mutation (one-point mutation), and fitness function (Friedman's lack-of-fit scoring function with two parameters) [33]. The selected variables entered a stepwise linear regression, as implemented in the MDL QSAR package. It was used in a forward mode with default value for *F*-to-enter (4.00) and *F*-to-remove (3.99).

4.5. Models assessment

Final models were assessed by explained variance (r^2), standard error of estimate (*SEE*), Fisher statistics (*F*) and leave-one-out cross-validated q^2.

Acknowledgement

Financial support of National Science Fund, Bulgaria (DMU 02/3-2009) is gratefully acknowledged.

References

[1] World Health Organization Global tuberculosis report, 2012, http://www.who.int/tb/publications/global_report/en/
[2] T.B. Stop, Partnership Working Group on New TB Drugs, 2009 http://www.stoptb.org/
[3] World Health Organization Initiative for Vaccine Research (IVR), BCG – the current vaccine for tuberculosis, http://www.who.int/vaccine_research/diseases/tb/vaccine_development/bcg/en/
[4] H.S. Cox, M. Morrow, P.W. Deutschmann, Long term efficacy of DOTS regimens for tuberculosis: systematic review, Br. Med. J. 336 (2008) 484–487.
[5] C. Lienhardt, A. Vernon, M.C. Raviglione, New drugs and new regimens for the treatment of tuberculosis: review of the drug development pipeline and implications for national programmes, Curr. Opin. Pulm. Med. 16 (2010) 186–193.
[6] D.C. Young, Computational Drug Design, John Wiley & Sons, Inc., Hoboken, NJ, 2009.
[7] Y. Koseki, S. Aoki, Computational medicinal chemistry for rational drug design: identification of novel chemical structures with potential anti-tuberculosis activity, Curr. Top. Med. Chem. 14 (2014) 176–188.
[8] X. Lu, B. Wan, S.G. Franzblau, Q. You, Design, synthesis and anti-tubercular evaluation of new 2-acylated and 2-alkylated amino-5-(4-(benzyloxy)phenyl)thiophene-3carboxylic acid derivatives. Part 1, Eur. J. Med. Chem. 46 (2011) 3551–3563.
[9] A. Manvar, A. Bavishi, A. Radadiya, J. Patel, V. Vora, N. Dodia, K. Rawal, A. Shah, Diversity oriented design of various hydrazides and their in vitro evaluation against *Mycobacterium tuberculosis* H37Rv strains, Bioorg. Med. Chem. Lett. 21 (2011) 4728–4731.
[10] C.R. Gomes, M. Moreth, D. Cardinot, V. Kopke, W. Cunico, M.C. da Silva Lourenco, M.V. de Souza, Synthesis and antimycobacterial activity of novel amino alcohols containing central core of the anti-HIV drugs lopinavir and ritonavir, Chem. Biol. Drug Des. 78 (2011) 1031–1034.
[11] N. Dwivedi, B.N. Mishra, V.M. Katoch, 2D-QSAR model development and analysis on variant groups of anti-tuberculosis drugs, Bioinformation 7 (2011) 82–90.
[12] P. De, K. De, D. Veau, F. Bedos-Belval, S. Chassaing, M. Baltas, Recent advances in the development of cinnamic-like derivatives as antituberculosis agents, Expert Opin. Ther. Pat. 22 (2012) 155–168.
[13] A. Speck-Plance, V.V. Kleandrova, F. Luan, M.N. Cordeiro, In silico discovery and virtual screening of multi-target inhibitors for proteins in *Mycobacterium tuberculosis*, Comb. Chem. High Throughput Screen. 15 (2012) 666–673.
[14] R.V. Bueno, N.R. Toledo, B.J. Neves, R.C. Braga, C.H. Andrade, Structural and chemical basis for enhanced affinity to a series of mycobacterial thymidine monophosphate kinase inhibitors: fragment-based QSAR and QM/MM docking studies, J. Mol. Model. 19 (2013) 179–192.
[15] A. Speck-Plance, V.V. Kleandrova, F. Luan, M.N. Cordeiro, New insights towards the discovery of antibacterial agents: multi-tasking QSBER model for the simultaneous prediction of anti-tuberculosis activity and toxicological profiles of drugs, Eur. J. Pharm. Sci. 48 (2013) 812–818.
[16] E.J. North, M.S. Scherman, D.F. Bruhn, J.S. Scarborough, M.M. Maddox, V. Jones, A. Grzegorzewicz, L. Yang, T. Hess, C. Morisseau, M. Jackson, M.R. McNeil, R.E. Lee, Design, synthesis and anti-tuberculosis activity of 1-adamantyl-3-heteroaryl ureas with improved in vitro pharmacokinetic properties, Bioorg. Med. Chem. 21 (2013) 2587–2599.
[17] A. Manvar, V. Khedkar, J. Patel, V. Vora, N. Dodia, G. Patel, E. Coutinho, A. Shah, Synthesis and binary QSAR study of antitubercular quinolylhydrazides, Bioorg. Med. Chem. Lett. 23 (2013) 4896–4902.
[18] M. Pieroni, B. Wan, S. Cho, S.G. Franzblau, G. Costantino, Design, synthesis and investigation on the structure–activity relationships of N-substituted 2-aminothiazole derivatives as antitubercular agents, Eur. J. Med. Chem. 72 (2014) 26–34.
[19] T.C. Ramalho, M.S. Caitano, D. Josa, G.P. Luz, E.A. Freitas, E.F. da Cunha, Molecular modeling of *Mycobacterium tuberculosis* dUTpase: docking and catalytic mechanism studies, J. Biomol. Struct. Dyn. 28 (2011) 907–917.
[20] A. Breda, P. Machado, L.A. Rosado, A.A. Souto, D.S. Santos, L.A. Basso, Pyrimidin-2(1H)-ones based inhibitors of *Mycobacterium tuberculosis* orotate phosphoribosyltransferase, Eur. J. Med. Chem. 54 (2012) 113–122.
[21] Y. Maharaj, M.E. Soliman, Identification of novel gyrase B inhibitors as potential anti-TB drugs: homology modeling, hybrid virtual screening and molecular dynamics simulations, Chem. Biol. Drug Des. 82 (2013) 2015–2215.
[22] A. Arvind, V. Jain, P. Saravanan, C.G. Mohah, Uridine monophosphate kinase as potential target for tuberculosis: from target to lead identigication, Interdiscip. Sci. 5 (2013) 296–311.
[23] G. Stavrakov, V. Valcheva, I. Philipova, I. Doytchinova, Novel camphene-based anti-tuberculosis agents with nanomolar activity, Eur. J. Med. Chem. 70 (2013) 372–379.
[24] L.B. Kier, L.H. Hall, Intermolecular accessibility: the meaning of molecular connectivity, J. Chem. Inf. Comput. Sci. 40 (2000) 792–795.
[25] MDL QSAR version 2.2, MDL Information Systems, Inc., San Leandro, USA.
[26] G. Stavrakov, I. Philipova, V. Valcheva, G. Momekov, Synthesis and antimycobacterial activity of novel camphane-based agents, Bioorg. Med. Chem. Lett. 24 (2014) 165–167.
[27] J. Ipaktschi, Reduction of oximes with sodium borohydride in the presence of transition metal compounds, J. Chem. Ber. 117 (1984) 856–858.
[28] R.M. Carman, K.L. Greenfield, The endo- and exo-1, 7,7-trimethylbicyclo[2.2.1] heptan-2-amines (bornan-2-amines) and their acetamides, Aust. J. Chem. 37 (1984) 1785–1790.
[29] G. Canetti, W. Fox, A. Khomenko, H.T. Mahler, N.K. Menon, D.A. Mitchinson, N. Rist, N.A. Smelev, Advances in techniques of testing mycobacterial drug sensitivity and the use of sensitivity tests in tuberculosis control programmes, Bull. World Heath Organ. 41 (1969) 21–43.
[30] L.H. Hall, L.B. Kier, Molecular connectivity chi indices for database analysis and structure–property modeling, in: J. Devillers, A. Balaban (Eds.), Topological Indices and Related Descriptors in QSAR and QSPR, Gordon and Breach, London, UK, 1999.
[31] L.H. Hall, L.B. Kier, Electrotopological state: structure modeling for QSAR and database analysis, in: J. Devillers, A. Balaban (Eds.), Topological Indices and Related Descriptors in QSAR and QSPR, Gordon and Breach, London, UK, 1999.
[32] R. Leardi, R. Boggia, M. Terrile, Genetic algorithms as a strategy for feature selection, J. Chemom. 6 (1992) 267–281.
[33] J. Friedman, Multivariate Adaptive Regression Splines. Technical Report No. 102, Laboratory for Computational Statistics, Department of Statistics, Stanford University, Stanford, CA, 1988.